

Article

Development of an Interaction Assay between Single-Stranded Nucleic Acids Trapped with Silica Particles and Fluorescent Compounds

T. Isoda ^{1,*} and R. Maeda ²

¹ Department of Life and Environment Engineering, Faculty of Environmental Engineering, University of Kitakyushu, 1-1, Hibikino, Wakamatsu, Kitakyushu 808-0135, Japan

² Department of Life and Environment Engineering, Graduate School of Environmental Engineering, University of Kitakyushu, 1-1, Hibikino, Wakamatsu, Kitakyushu 808-0135, Japan; E-Mail: s1mab008@eng.kitakyu-u.ac.jp

* Author to whom correspondence should be addressed; E-Mail: isoda@env.kitakyu-u.ac.jp; Tel.: +81-93-695-3285; Fax: +81-93-695-3377.

Received: 13 July 2012; in revised form: 7 August 2012 / Accepted: 21 August 2012 /

Published: 5 September 2012

Abstract: Biopolymers are easily denatured by heating, a change in pH or chemical substances when they are immobilized on a substrate. To prevent denaturation of biopolymers, we developed a method to trap a polynucleotide on a substrate by hydrogen bonding using silica particles with surfaces modified by aminoalkyl chains ([A-AM silane]/SiO₂). [A-AM silane]/SiO₂ was synthesized by silane coupling reaction of N-2-(aminoethyl)-3-aminopropyltrimethoxysilane (A-AM silane) with SiO₂ particles with a diameter of 5 μm at 100 °C for 20 min. The surface chemical structure of [A-AM silane]/SiO₂ was characterized by Fourier transform infrared spectroscopy and molecular orbital calculations. The surface of the silica particles was modified with A-AM silane and primary amine groups were formed. [A-AM silane]/SiO₂ was trapped with single-stranded nucleic acids [(Poly-X; X = A (adenine), G (guanine) and C (cytosine))] in PBS solution at 37 °C for 1 h. The single-stranded nucleic acids were trapped on the surface of the [A-AM silane]/SiO₂ by hydrogen bonding to form conjugated materials. The resulting complexes were further conjugated by derivatives of acridine orange (AO) as fluorescent labels under the same conditions to form [AO:Poly-X:A-AM silane]/SiO₂ complexes. Changes in the fluorescence intensity of these complexes originating from interactions between the

single-stranded nucleic acid and aromatic compounds were also evaluated. The change in intensity displayed the order [AO: Poly-G: A-AM silane]/SiO₂ > [AO:Poly-A:A-AM silane]/SiO₂ >> [AO:Poly-C:A-AM silane]/SiO₂. This suggests that the single-stranded nucleic acids conjugated with aminoalkyl chains on the surfaces of SiO₂ particles and the change in fluorescence intensity reflected the molecular interaction between AO and the nucleic-acid base in a polynucleotide.

Keywords: nucleic acid; polynucleotide; assay; fluorescence; cellstain-AO

Abbreviations

A-AM silane: N-2-aminoethyl-3-aminopropyltrimethoxysilane (KBM-603, Shin-Etsu Chemical Co., Ltd., Tokyo, Japan).

B-AM silane: N-phenyl-3-aminopropyltrimethoxysilane (KBM-573, Shin-Etsu Chemical Co., Ltd., Tokyo, Japan).

[A-AM silane]/SiO₂: silica particles surface-modified with aminoalkyl chains.

[X-AM silane]/SiO₂: X = A: amino group and B: phenyl group.

Poly-X: polynucleotides-X, X = A (adenine), G (guanine) and C (cytosine).

AO: derivatives of acridine orange (Cellstain-AO; Dojindo Laboratories, Kumamoto, Japan.).

FITC: fluorescein isothiocyanate.

MO: Molecular orbital.

HOMO: highest occupied molecular orbital.

LUMO: lowest unoccupied molecular orbital.

1. Introduction

Recently, protein-function arrays and/or functional proteomics have attracted attention as a novel biotechnology that can obtain information about the interaction between a protein and another protein, a nucleotide or a small molecule. To construct this assay, it is necessary to immobilize many kinds of protein on a substrate. Conjugation of proteins and biopolymers with a substrate is a breakthrough technology for the development of protein-function arrays. Many studies of surface chemistry related to biomolecules have been reported.

Physical adsorption has been widely used as an immobilization method [1,2]. When a solution containing protein is added dropwise onto a nitrocellulose [1] or polyvinylidene fluoride membrane [2], the protein is immobilized on the membrane surface by hydrophobic interactions; however, the adhesion is weak. Schreibe *et al.* chemically bonded bovine serum albumin (BSA) on a glass substrate using aldehyde and then further immobilized other proteins on this BSA-modified surface [3]. The carboxyl groups of the glutamate residues in BSA were converted to an active ester, which bonded to amino groups in other proteins. A different method was reported by Zhu *et al.* [4] who immobilized proteins on a glass substrate modified with epoxy groups through chemical bonding to amino groups in the proteins.

Jung and coworkers immobilized peptides on the surface of a gold electrode coated with a

self-assembled membrane (SAM) [5]. In this case, the end of the SAM, which consisted of *p*-hydroxyazobenzene groups, was changed to *p*-quinonimine by electrolysis and oxidation. Cysteine residues in the peptide reacted with *p*-quinonimine by 1,4-Michael addition. Meanwhile, Byeon *et al.* immobilized antibodies on a substrate through condensation of hydrazine and aldehyde in the presence of aniline as a catalyst [6].

We have developed polystyrene (PS) microbeads, modified with schizophyllan (SPG) or polysaccharide [7]. The molecular weight of SPG was about 150,000 and its end unit was modified with an amino group. The amino group of SPG bound covalently to a carboxyl group on the support surface to form the composite PS-SPG [8]. Nucleic acids were preferentially adsorbed in particular, and could be detected by the microelectrode when the adsorbent consisted of PS microbeads with a SPG-modified surface.

A different protein immobilization method involves using a protein implanted with a ligand that acts as a tag [9]. The tag consisted of a continuous sequence of seven to eight histidine residues and could bond to a Ni complex on the surface of a substrate. An advantage of this method is that all proteins coordinate in the same direction, which prevents deactivation. It has been reported that 80% of 5800 kinds of yeast proteins maintained their activity when immobilized using this method. Katayama *et al.* also reported immobilization of an estrogen-receptor [10] and transcription factor [11] on a gold electrode using this method.

However, basic research investigating conjugation of a protein or biopolymer to a solid surface is not always suitable for application to protein-function array technology, although various methods have been developed. In particular, most immobilization methods use covalent bonding and/or hydrophilic interactions between a protein or biopolymer and a solid surface. There are few examples of immobilization methods using hydrogen bonding.

In this study, we fabricated silica particles with surfaces that were modified by aminoalkyl chains. The amino groups introduced on the surface can interact with single-stranded nucleic acids through hydrogen bonding, resulting in a conjugate between a polynucleotide and inorganic material. The single-stranded nucleic acid trapped to the silica particle was further interacted by an acridine orange derivative as a fluorescent label, allowing changes in fluorescence intensity originating from interactions between the single-stranded nucleic acid and aromatic compounds to be investigated. The affinity of an acridine orange derivative to interact with single-stranded nucleic acid trapped on the silica particle is discussed.

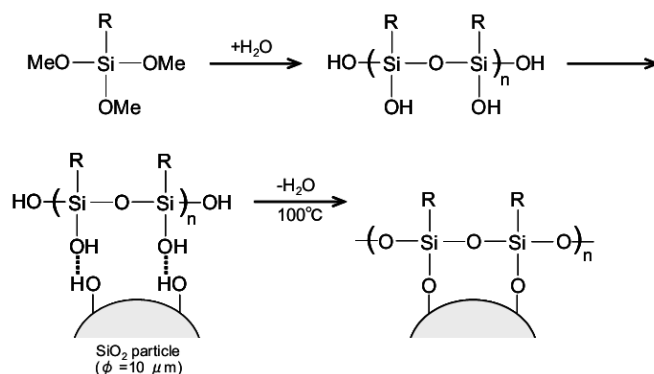
2. Experimental Procedures

2.1. Preparation of SiO₂ Particles Modified with Aminoalkyl Chains

Reaction mechanism of silane coupling on a SiO₂ surface is shown in Figure 1 [12]. Hypersil silica (GL Science Co., Ltd., Japan; particle diameter: 5 μm) was used as SiO₂ particles. Two kinds of silane derivatives were used; N-2-aminoethyl-3-aminopropyltrimethoxysilane (KBM-603; abbreviated to A-AM silane) and N-phenyl-3-aminopropyltrimethoxysilane (KBM-573; abbreviated to B-AM silane). Both chemicals were purchased from Shin-Etsu Chemical Co., Ltd., Japan. The structure was shown in Figure 2. Silanol derivatives were formed by hydrolysis of silane derivatives in aqueous solutions containing 2%, 20% and 40% A-AM or B-AM silane at 20 °C for 30 min. The silane coupling reaction of each silanol derivative was carried out at 100 °C for 10 min in a Teflon beaker. The hydroxyl groups of silanol derivatives were covalently bonded to hydroxyl groups on the SiO₂ surface via condensation

reaction to form SiO₂ particles modified with aminoalkyl chains, [X-AM silane]/SiO₂ (X = A: amino group and B: phenyl group).

Figure 1. Reaction mechanism of silane coupling on a SiO₂ particle.



2.2. Analysis of Surface Chemical Structure

Functional groups on the surface of the aminoalkylated SiO₂ particles were qualitatively analyzed by Fourier transform infrared spectroscopy (FT-IR; Perkin Elmer, USA). Spectra were recorded using KBr discs containing 1 to 5 wt% sample. The substitution of aminoalkyl chains on the SiO₂ surface was further confirmed by fluorescence labeling. The reaction scheme is also illustrated in Figure 2. Each sample (5 mg) and fluorescein isothiocyanate (FITC; 2.5 $\mu\text{g}/\text{mL}$, Dojindo Laboratories Co., Ltd., Japan) in PBS solution was stirred at 20 °C for 5 min. The sample was washed twice with distilled water (DW) to give labeled aminoalkylated SiO₂ particles [FITC:X-AM silane]/SiO₂ (X = A: amino group and B: phenyl group). Fluorescence intensity was determined using a fluorescence microscope (U-RFLT50, Olympus, Japan) at a wavelength of 520 nm. [FITC:X-AM silane]/SiO₂ (5 mg) was dispersed in DW (300 μL) and placed in one well of a culture slide (well size: 10 mm², BD Co., Ltd., USA). After deposition of the particle solution for 5 min, images were obtained at 15 arbitrary points in the cell and analyzed to determine average intensity.

2.3. Trapping Procedure of Single-Stranded Nucleic Acids Using Aminoalkylated SiO₂ Particles

A flow chart outlining the preparation of complexes of single-stranded nucleic acid trapped with [A-AM silane]/SiO₂ and fluorescence compounds is shown in Figure 3. The schematic illustration was also shown in Figure 4. Single-stranded nucleic acids composed of only cytosine, adenine or guanine (poly-C, poly-A and poly-G, respectively; Wako Chemicals, Japan) were used. Solutions of poly-X (X = C, A or G, 12.5 mg/mL) in PBS were prepared. A mixture of each poly-X solution and [A-AM silane]/SiO₂ (5 mg) was incubated at 37 °C for 1 h. The particles were separated by centrifugation and then washed to give complexes of polynucleotide and [A-AM silane]/SiO₂ ([Poly-X:A-AM silane]/SiO₂; Figure 4a). An acridine orange derivative (named AO) was used as a fluorescent label (Cellstain-AO; Dojindo Laboratories Co., Ltd., Japan). The chemical structure is shown in Figure 4b. When AO interacts with phosphate group and/or nucleobase in single-stranded polynucleotides, such as complementary DNA or messenger RNA, the molecules are arranged in a random order. Some associate with AO in the

single-stranded polynucleotide, giving rise to red fluorescence ($\lambda_{\text{max}} = 650 \text{ nm}$) [13,14]. [Poly-X:A-AM silane]/SiO₂ (5 mg) was dispersed in AO in PBS solution (0.1–10 $\mu\text{g/mL}$) and incubated at 37 °C for 1 h. The particles were separated by centrifugation and washed to give fluorescent-labeled [Poly-X:A-AM silane]/SiO₂ particles ([AO:Poly-X:A-AM silane]/SiO₂; Figure 4c). Fluorescence intensity was measured using a fluorescence microscope at a wavelength of 640 nm using the method described in the previous section.

Figure 2. Reaction scheme of fluorescence labeling after preparation of two kinds of silane coupling on SiO₂ particles.

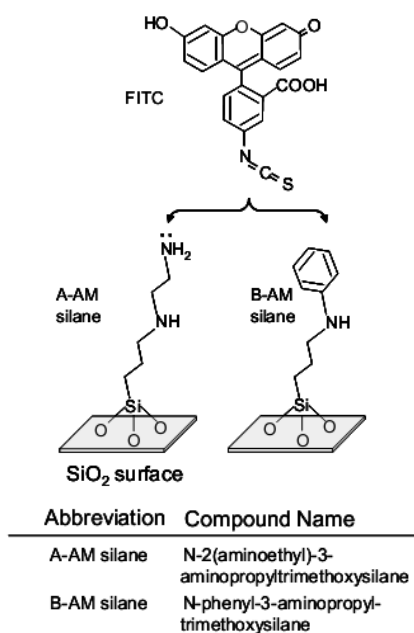


Figure 3. Flow chart outlining the preparation of [AO:Poly-X:A-AM silane]/SiO₂ complexes for fluorescence analysis.

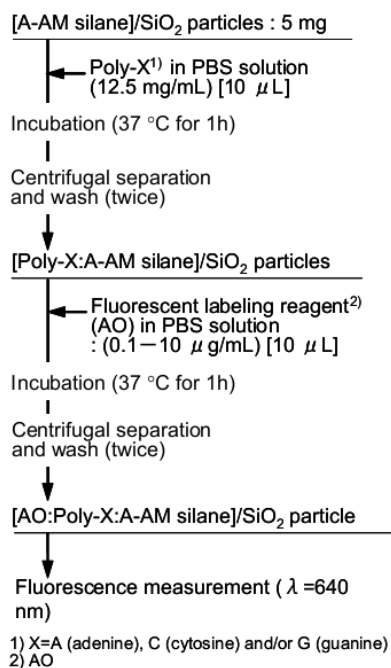
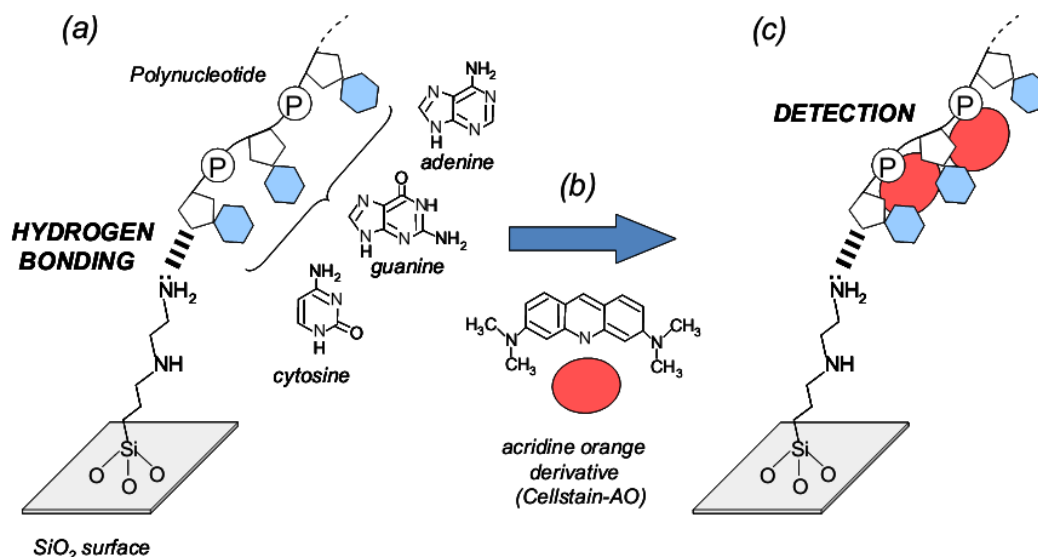


Figure 4. The schematic illustration of interaction assay between single-stranded nucleic acids trapped with silica particles and fluorescent compounds. (a) Stage of nucleotide trapping on aminoalkylated SiO₂ particles; (b) structure of cellstain-AO as fluorescent compound; (c) and conjugation stage of cellstain-AO with single-stranded nucleic acids.



2.4. Molecular Orbital Calculations of Surface Model Structure of Aminoalkylated SiO₂, Polynucleotides and Fluorescent Compound

Molecular orbital (MO) calculations to obtain a surface model structure of aminoalkylated SiO₂, polynucleotides and fluorescent compound were carried out using commercial software (MOPAC Vr.3, Fujitsu Co., Japan) with the PM3 method [15]. A-AM silanol as a coupling precursor and a Si₄O₄(OH)₁₀ cluster combined with A-AM silanol as a surface model of a SiO₂ particle is shown in Figures 6a and b, respectively (silicon and oxygen atoms are shown as yellow and red color).

The geometry of each molecule was optimized, and then a hydroxyl group in each molecule was bonded to silica. The geometry was optimized again to generate an [A-AM silane]/SiO₂ cluster. Simulated FT-IR spectra were determined by vibration calculation of the [A-AM silane]/SiO₂ cluster using the PM3 method. Polynucleotide composed of three units of nucleobase and cellstain-AO molecule as a fluorescent compound was also calculated by the method described above.

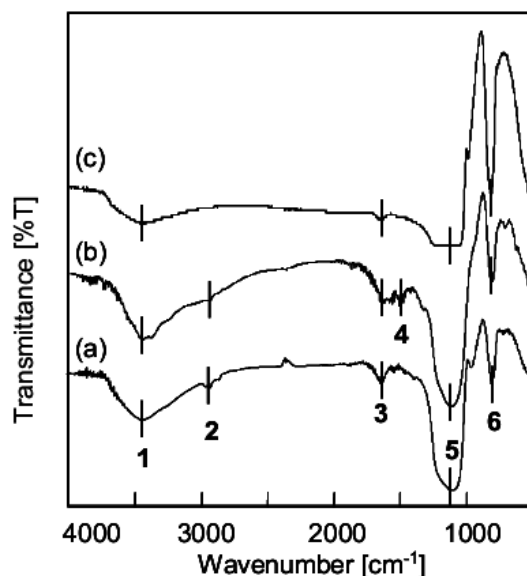
3. Results

3.1. Chemical Structure of Aminoalkylated SiO₂ Surface

FT-IR spectra of the surface of SiO₂ particles after aminosilane coupling are presented in Figure 5. Here, SiO₂ particles treated with X-AM silane (n%) are abbreviated as [X-AM silane (n%)]/SiO₂. Figure 5a shows an FT-IR spectrum of [A-AM silane (2%)]/SiO₂. The peaks labeled 1 and 5 are assigned to -OH ($\nu = 3385\text{--}3418\text{ cm}^{-1}$) and Si-O-Si bonds ($\nu = 1090\text{--}1120\text{ cm}^{-1}$) in SiO₂. Peaks 2 and 3 are assigned to -CH₂- ($\nu = 2911\text{--}2929\text{ cm}^{-1}$) and -NH₂ or -CH₂-NH₂ bonds ($\nu = 1568\text{--}1634\text{ cm}^{-1}$), respectively. Figure 5b shows an FT-IR spectrum of [A-AM silane (40%)]/SiO₂, which contains Peak 4 assigned to -CH₂- bonds ($\nu = 1471\text{ cm}^{-1}$). These results suggest that A-AM silane has been introduced onto the surface of

SiO₂. Figure 5c shows an FT-IR spectrum of [B-AM silane (2%)]/SiO₂ for comparison. In this case, peak 3 almost disappeared because there is no amino group in B-AM silane.

Figure 5. FT-IR spectra of the surface of SiO₂ particles following amino-silane coupling. SiO₂ particles treated with X-AM silane (n%) are abbreviated as [X-AM silane (n%)]/SiO₂. (a) [A-AM silane (2%)]/SiO₂; (b) [A-AM silane (40%)]/SiO₂; (c) [B-AM silane (2%)]/SiO₂.



Peak	1	2	3	4	5	6
Wavenumber [cm ⁻¹]	3385-3418	2911-2929	1568-1634	1471	1090-1120	790
Functional group	-OH	-CH ₂ -	NH ₂ or -CH ₂ -NH ₂	-CH ₂ -	Si-O-Si	unknown

Measured and calculated FT-IR spectra are presented in Figure 6, where a spectrum measured for [A-AM silane (40%)]/SiO₂ (Figure 6c) is compared to simulated spectra for A-AM silanol (Figure 6a) and [A-AM silane]/SiO₂ clusters (Figure 6b).

Six major peaks were obtained from the vibrational calculation for A-AM silanol, as shown in Figure 6a. Peaks 2, 4, 6 and 7 are assigned to -CH₂- bonds ($\nu = 3022, 1376, 1160$ and 779 cm^{-1}), while peaks 1 and 3 are assigned to -NH₂ bonds ($\nu = 3,522$ and $1,670 \text{ cm}^{-1}$). Except for peak 5, these correspond to the calculated spectrum for an [A-AM silane]/SiO₂ cluster (Figure 6b). Peak 5 for the cluster is consistent with vibration of Si-O-Si bonds ($\nu = 965 \text{ cm}^{-1}$). The wavenumbers of the simulated peaks are close to those in an FT-IR spectrum measured for [A-AM silane (40%)]/SiO₂ (Figure 6c).

Figure 6. Simulated FT-IR spectra of (a) A-A silanol; and (b) Si₄O₄(OH)₁₀ cluster combined with A-AM silane; (refer to Figure 2 for structures) compared to (c) measured FT-IR spectrum of [A-AM silane (40%)]/SiO₂.

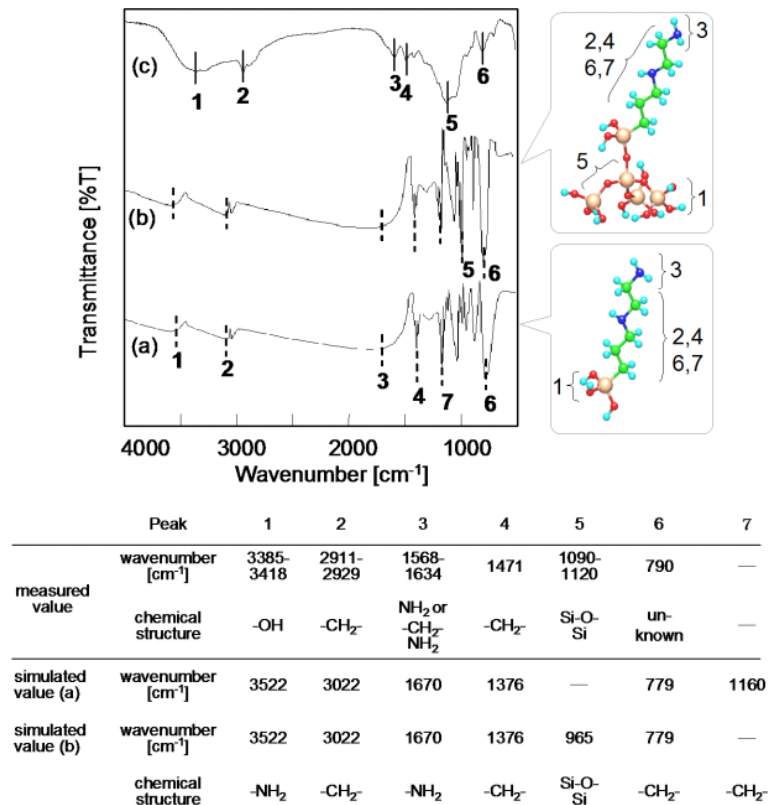
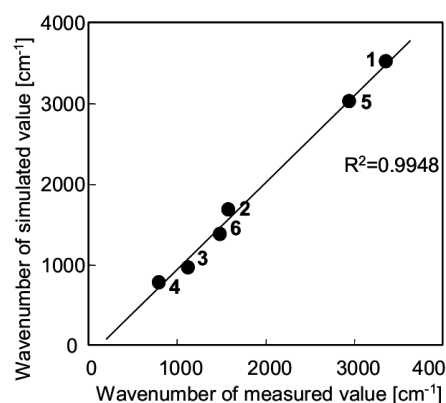


Figure 7 shows the relationship between the results of the vibrational calculation for [A-AM silane]/SiO₂ cluster as a model molecule (Figure 6b) and the measured data for [A-AM silane (40%)]/SiO₂ (Figure 6c). There is a good correlation between the simulated and measured peaks. Fitting the data with a linear approximation gave a correlation coefficient of 0.9948. This suggests that the structure of the aminoalkyl chains on the SiO₂ surface is similar to the structure predicted for the [A-AM silane]/SiO₂ cluster.

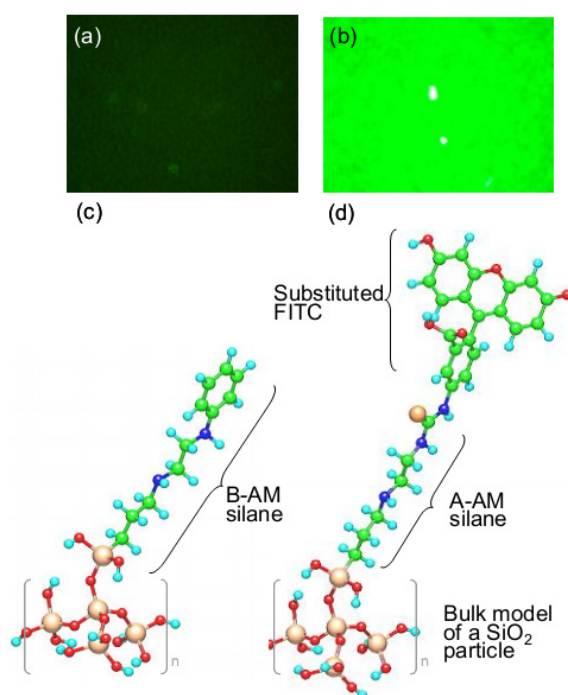
Figure 7. Relationship between the vibrational calculation result for a Si₄O₄(OH)₁₀ cluster combined with A-AM silane (structure given in Figure 6b) and measured FT-IR spectrum of [A-AM silane (40%)]/SiO₂.



3.2. Orientation of Aminoalkyl Chains on the SiO₂ Surface

Figure 8 shows fluorescence microscope images of [B-AM silane (2%)]/SiO₂ (Figure 8a) and [A-AM silane (2%)]/SiO₂ (Figure 8b) after reaction with FITC, and models of the surface structure of both particles are shown in Figure 8c and d, respectively. The isothiocyanate group in FITC reacts selectively with a primary amine group, such as that in A-AM silane to form a thiourea bond between both functional groups.

Figure 8. Fluorescence microscope images of (a) [B-AM silane (2%)]/SiO₂, and (b) [A-AM silane (2%)]/SiO₂ after reaction with FITC. Models of the surface structure are shown in (c) and (d), respectively.



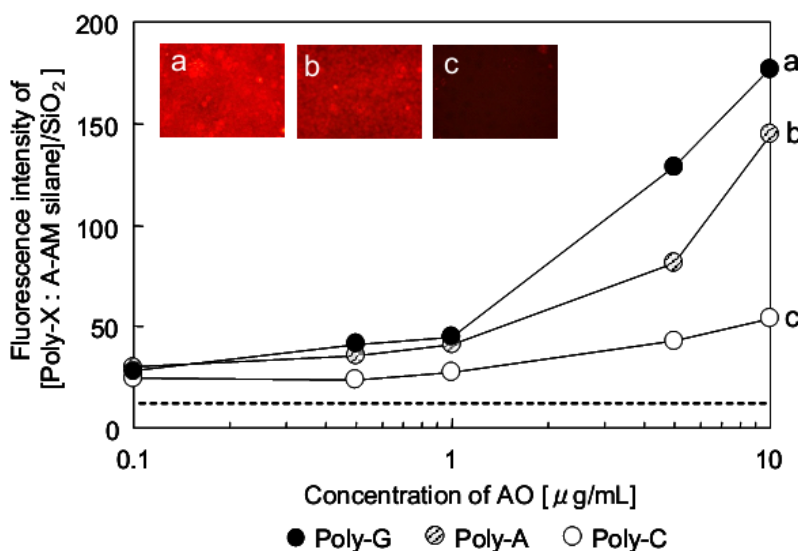
The intensity of green fluorescence at $\lambda = 520$ nm from the samples is clearly different. [A-AM silane (2%)]/SiO₂ treated with FITC shows a relative fluorescence intensity of 250 ± 4 , whereas for [B-AM silane (2%)]/SiO₂ it is 50 ± 4 . These results suggest that the terminally-connected phenyl group in B-AM silane and amino group in A-AM silane are oriented outwards on the surface of the SiO₂ particles.

3.3. Evaluation for Interaction of Single-stranded Nucleic Acids and Fluorescence Compound

Figure 9 shows the relationship between the concentration of AO and fluorescence intensity of Poly-X (X = guanine (G), adenine (A) and cytosine (C)) conjugated with [A-AM silane]/SiO₂. The schematic illustrations are also shown in Figure 4c. The fluorescence intensity of [A-AM silane]/SiO₂ treated with AO was measured to confirm their interaction. There was no interaction between AO and [A-AM silane]/SiO₂ (dotted line in Figure 9). The intensity of the red fluorescence at $\lambda = 640$ nm clearly depended on the type of polynucleotide in the conjugate. When different concentrations of AO were conjugated with [Poly-G:A-AM silane]/SiO₂, the relative fluorescence intensity of [AO:Poly-G:A-AM silane]/SiO₂ was 45 for 1 $\mu\text{g/mL}$, 129 for 5 $\mu\text{g/mL}$ and 177 for 10 $\mu\text{g/mL}$. When AO was conjugated with

[Poly-A: A-AM silane]/SiO₂, the fluorescence intensity of [AO: Poly-A: A-AM silane]/SiO₂ decreased compared with that of [AO: Poly-G: A-AM silane]/SiO₂ to 41 for 1 μg/mL, 81 for 5 μg/mL and 144 for 10 μg/mL. In the case of Poly-C, the fluorescence intensity of [AO:Poly-C:A-AM silane]/SiO₂ increased very little with concentration, showing an intensity of 27 for 1 μg/mL, 43 for 5 μg/mL and 54 for 10 μg/mL.

Figure 9. Relationship between concentration of AO and fluorescence intensity of [AO:Poly-X:A-AM silane]/SiO₂ [Poly-X: (a) X = guanine; (b) adenine; (c) cytosine].



The sensitivities of fluorescence intensity, *R*, of AO-labeled [Poly-X: A-AM silane]/SiO₂ conjugates are summarized in Table 1. For comparison, *R* of AO-labeled Poly-X ([AO: Poly-X]) are also summarized in Table 1. *R* was calculated using Equation (1):

$$R = (FL_{10} - FL_1)/(AO_{10} - AO_1) \tag{1}$$

Table 1. Sensitivities for fluorescence intensity of AO-labeled (a) [Poly-X:A-AM silane]/SiO₂ particles and (b) polynucleotides.

single-stranded nucleic acid	[AO:Poly-X:A-AM silane]/SiO ₂			[AO:Poly-X]		
	FL ₁₀	FL ₁	R ⁽¹⁾	FL ₁₀	FL ₁	R ⁽¹⁾
Poly-G	177	45	14.7	141	37	11.6
Poly-A	144	41	11.4	130	20	12.2
Poly-C	54	27	3.0	40	27	1.4

Note: (1) $R = (FL_{10} - FL_1)/(AO_{10} - AO_1)$.

In this instance, AO₁₀ and AO₁ were the concentrations of AO (μg/mL), while FL₁₀ and FL₁ were the fluorescence intensities when the concentrations of AO were 10 and 1 μg/mL, respectively. The difference of conjugation ability is particularly clear when single-stranded nucleic acids trapped with aminoalkylated SiO₂ are used. *R* of [Poly-X:A-AM silane]/SiO₂ increased in the order Poly-C < Poly-A < Poly-G. A similar trend was obtained for the [AO:Poly-X] complexes (amino-alkylated SiO₂ particle free). These results suggest that the conjugation of AO and

[Poly-X:A-AM silane]/SiO₂ is affected by the characteristics of the single-stranded nucleic acid. Based on the above results, it estimates that the difference of fluorescence intensity for AO and [Poly-X:A-AM silane]/SiO₂ was obtained clearly when the amount of each poly-X on amino-alkylated SiO₂ particle was the same.

3.4. Evaluation of the Interaction Between Nucleic-Acid Base in Nucleotides and Fluorescent Compound

Electron distributions of each model structure, which a surface model of a [A-AM silane]/SiO₂ cluster (Figure 6b), Poly-G, A or C with 3 units as the nucleotide fragment (Table 2) and fluorescence compound (Figure 4b), were calculated separately by the PM3 method.

Based on the results of electron distributions, the highest occupied molecular orbital (HOMO) is distributed on the terminal of each [A-AM silane]/SiO₂ cluster. This is because the nitrogen atom in an amino group has a lone electron pair. This result suggests that the surface of aminoalkylated SiO₂ has an electron-donating ability. In PBS solution (pH = 7), protonation of the primary amino group is an unfavorable reaction. It estimates there is little positive electric charge on the surface of the silica particle.

In contrast, it has been reported that AO as a fluorescence compound interacts with the phosphate group on the nucleotide by electrostatic interaction [13,14]. In accordance with the MO calculation result, the HOMO of AO, which contains a π electron, is also delocalized over the entire molecule. This suggests that AO also possesses electron-donating ability. It estimates that AO attaches to a phosphate group in the nucleotide by electrostatic interaction first, then the nucleobase around the AO interacts through its electron-donating ability.

Based on the results in Figure 9 and Table 1, the polynucleotides conjugate was trapped with aminoalkylated SiO₂ and was further conjugated with AO. This suggests that the polynucleotide behaves as an electron acceptor, and two vacant orbitals are necessary to interact with both aminoalkylated SiO₂ and AO. Based on the results of electron distributions, the lowest unoccupied molecular orbital (LUMO) and second LUMO of the nucleotide fragment are distributed on a central nucleotide and 5' end.

The interaction between the nucleotide and AO was evaluated using Equation (2):

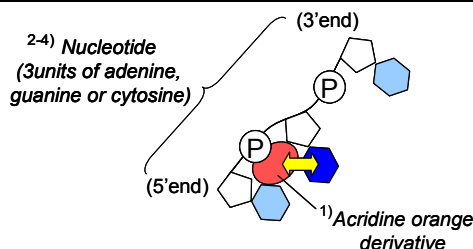
$$\Delta E \text{ (eV)} = E_N - E_A \quad (2)$$

In this instance, E_N is the energy level of the LUMO obtained from a MO calculation of each nucleotide, E_A is energy level of the HOMO obtained from the MO calculation of AO, and ΔE is an energy gap between each nucleotide conjugated and AO. Therefore, it is possible to determine an interaction parameter between two molecules using Frontier orbital theory [16].

A comparison of ΔE values is given in Table 2. ΔE decreased in the order of Poly-C > Poly-A > Poly-G, consistent with the results presented in Figure 9. This order reflects the interaction between fluorescent compounds and the nucleobase in single-stranded nucleic acids.

Table 2. Calculated energy levels for Poly-X⁽²⁻⁴⁾ and AO.

Calculated MO	AO ⁽¹⁾	Poly-C ⁽²⁾	Poly-A ⁽³⁾	Poly-G ⁽⁴⁾
HOMO [eV]	-7.695	-9.140	-8.840	-8.820
LUMO [eV]	-0.819	-0.345	-0.449	-0.482
ΔE	–	7.350	7.246	7.213



4. Discussion

In general, an adsorbent adsorbs a molecule through molecular interactions such as Van der Waals’ forces. As a result, there is no selectivity for adsorption of molecules. However, aminoalkylated SiO₂ is trapped with a single-strand nucleic acid that is further conjugated to AO through hydrogen bonding and charge-transfer interactions, respectively. Target molecules are immobilized arbitrarily on the surface of aminoalkylated SiO₂ by hydrogen bonding. Levit-Binnun *et al.* used a quantitative approach to explain the interaction between immobilized BSA on a solid surface and a biotinylated anti-BSA antibody as a target molecule [17]. They immobilized BSA on a substrate and then reacted it with a biotinylated anti-BSA antibody. The amounts of bonding m_D were evaluated by Equation (3):

$$m_D = m_v \alpha \beta \tag{3}$$

where α is the formation efficiency of a complex between immobilized protein P and target molecule M, β is the detection efficiency, and m_v is the number of M that can interact with P.

When M was labeled with a fluorescent compound, β became 1, allowing Equation (3) to be simplified to:

$$m_D = m_v \alpha \tag{4}$$

where α is an eigenvalue that mainly depends on the surface coverage of functional group σ , the immobilization rate of P on the surface ρ and the affinity between P and M, K_d .

In this study, P and M correspond to Poly-X and AO, respectively, and m_D was approximated using Equation (4). M was constant, therefore, it is estimated that m_v was also constant. σ was 100% because the SiO₂ surface saturated with A-AM silane during coupling. Experimental results showed that ρ did not depend on the type of polynucleotide, so was a constant. As a result, α did not depend on ρ .

In contrast, K_d was significantly influenced by the type of polynucleotide, which is consistent with both experimental and simulation results. This suggests that the surface properties of aminoalkylated SiO₂ strongly reflect chemical properties such as the electron density on molecule P that can conjugate to the surface.

5. Conclusions

In this study, single-stranded nucleic acids were trapped on a solid surface using hydrogen bonding, which prevented denaturation of the biopolymers. The surface of silica particles was modified with A-AM silane to form primary amines that interact with single-stranded nucleic acids through hydrogen bonding to form conjugated materials in a short time. This complex was then selectively interacted with a fluorescence labeling reagent such as an acridine orange derivative. Changes in fluorescence intensity depended on the polynucleotide with the order poly-guanine > poly-adenine >> poly-cytosine. This suggests the different fluorescence intensities reflected the different molecular interactions between the acridine orange derivative and nucleic-acid base in polynucleotides. The results of MO calculations suggest that the surface properties of aminoalkylated SiO₂ strongly reflect its chemical properties, such as the electron density of a molecule that can conjugate to the surface.

Acknowledgement

This work was supported by the Japan Society for the Promotion of Science under Grant-in-Aid for Scientific Research [Scientific Research (C): 23560409]. We acknowledge Shiho Kabano, marketing department at Dojindo Laboratories, Japan, for her assistance with the production of Cellstain-AO acridine derivatives. We also thank the Shin-Etsu Chemical Co., Ltd., Japan, for providing silane compounds KBM-603 and KBM-573.

References

1. Ge, H. UPA, a universal protein array system for quantitative detection of protein-protein, protein-DNA, protein-RNA and protein-ligand interactions. *Nucleic Acid Res.* **2000**, *28*, e3.
2. Holt, L.J.; Bussow, K.; Walter, G.; Tomlinson, I.M. By-passing selection: Direct screening for antibody-antigen interactions using protein arrays. *Nucleic Acid Res.* **2000**, *28*, E72.
3. MacBeath, G.; Schreiber, S.L. Printing proteins as microarrays for high-throughput function determination. *Science* **2000**, *289*, 1760–1763.
4. Zhu, H.; Klemic, J.F.; Chang, S.; Bertone, P.; Casamayor, A.; Klemic, K.G.; Smith, D.; Gerstein, M.; Reed, M.A.; Snyder, M. Analysis of yeast protein kinases using protein chips. *Nat. Genetics.* **2000**, *26*, 283–289.
5. Jung, H.J.; Hwang, I.; Kim, B.J.; Min, H.; Yu, H.; Lee, T.G.; Chung, T.D. Selective and direct immobilization of cysteinyl biomolecules by electrochemical cleavage of azo linkage. *Langmuir* **2010**, *26*, 15087–15091.
6. Byeon, J.-Y.; Limpoco, F.T.; Bailey, R.C. Efficient bioconjugation of protein capture agents to biosensor surfaces using aniline-catalyzed hydrazone ligation. *Langmuir* **2010**, *26*, 15430–15435.
7. Kimura, T.; Koumoto, K.; Mizu, M.; Sakurai, K.; Shinkai, S. Polysaccharide-polynucleotide Interaction (XI); Novel separation system of RNAs by using schizophyllan appended column. *Chem. Lett.* **2002**, *12*, 1240–1241.
8. Isoda, T.; Takahara, N.; Imanaga, H.; Imamura, R.; Hasegawa, S.; Noguchi, K.; Kimura, T. Measurement of non-electrolyte concentrations in an ion solution using a micro-electrode. *Sens. Actuators B* **2006**, *120*, 1–9.

9. Zhu, H.; Bilgin, M.; Bangham, R.; Hall, D.; Casamayor, A.; Bertone, P.; Lan, N.; Jansen, R.; Bidlingmaier, S.; Houfek, T.; Mitchell, T.; Miller, P.; Dean, R.A.; Gerstein, M.; Snyder, M. Global analysis of protein activities using proteome chips. *Science* **2001**, *293*, 2101–2105.
10. Murata, M.; Nakayama, M.; Irie, H.; Yakabe, K.; Fukuma, K.; Katayama, Y.; Maeda, M. Novel biosensor for the rapid measurement of estrogen based on a ligand-receptor interaction. *Anal. Sci.* **2001**, *17*, 387–390.
11. Murata, M.; Yano, K.; Kuroki, S.; Suzutani, T.; Katayama, Y. Protein-immobilized electrode for rapid and convenient sensing of thyroid hormone receptor-ligand interaction. *Anal. Sci.* **2003**, *19*, 1569–1573.
12. Arkles, B. Hybrid polymers in the marketplace: Mix and match molecular building blocks to create better contact lenses, smoother-sailing ships, slippery surfaces, and more. *Chem. Tech.* **1999**, *29*, 7–14.
13. Miyoshi, M.; Hara, K.; Yokoyama, I.; Tomita, G.; Taylor, I.W.; Milthorpe, B.K. An evaluation of DNA fluorochromes, staining techniques, and analysis for flow cytometry. I. Unperturbed cell populations. *J. Histochem. Cytochem.* **1980**, *28*, 1224–1232.
14. El-Naggar, A.K.; Batsakis, J.G.; Teague, K.; Garnsey, L.; Barlogie, B. Single- and double-stranded RNA measurements by flow cytometry in solid neoplasms. *Cytometry* **1991**, *12*, 330–335.
15. Stewart, J.J.P. MOPAC: A semiempirical molecular orbital program. *J. Comput. Aided Mol. Des.* **1990**, *4*, 1–103.
16. Fukui, K.; Yonezawa, T.; Shingu, H. A molecular orbital theory of reactivity in aromatic hydrocarbons. *J. Chem. Phys.* **1952**, *20*, 722–725.
17. Levit-Binnun, N.; Lindner, A.B.; Zik, O.; Eshhar, Z.; Moses, E. Quantitative detection of protein arrays. *Anal. Chem.* **2003**, *75*, 1436–1441.

© 2012 by the authors; licensee MDPI, Basel, Switzerland. This article is an open access article distributed under the terms and conditions of the Creative Commons Attribution license (<http://creativecommons.org/licenses/by/3.0/>).